Voltage Control of the Resonance Frequency of Dielectric Electroactive Polymer (DEAP) Membranes

Philippe Dubois, Samuel Rosset, Muhamed Niklaus, Massoud Dadras, and Herbert Shea, *Member, IEEE*

***Abstract*—We report on the characterization, active tuning, and modeling of the first mode resonance frequency of dielectric electroactive polymer (DEAP) membranes. Unlike other resonance frequency tuning techniques, the tuning procedure presented here requires no external actuators or variable elements. Compliant electrodes were sputtered or implanted on both sides of 20–35-μm-thick and 2–4-mm-diameter polydimethylsiloxane membranes. The electrostatic force from an applied voltage adds compressive stress to the membrane, effectively softening the device and reducing its resonance frequency, in principle to zero at the buckling threshold. A reduction in resonance frequency up to 77% (limited by dielectric breakdown) from the initial value of 1620 Hz was observed at 1800 V for ion-implanted membranes. Excellent agreement was found between our measurements and an analytical model we developed based on the Rayleigh–Ritz theory. This model is more accurate in the tensile domain than the existing model for thick plates applied to DEAPs. By varying the resonance frequency of the membranes (and, hence, their compliance), they can be used as frequency-tunable attenuators. The same technology could also allow the fine-tuning of the resonance frequencies in the megahertz range of devices made from much stiffer polymers. [2007-0202]**

***Index Terms*—Artificial muscle, dielectric elastomer actuator, dielectric electroactive actuator (DEA), dielectric electroactive polymer (DEAP), electroactive polymer (EAP), electrode compliance, ion implantation, membrane, resonance frequency tuning, tunable resonators.**

I. Introduction

THE MEMS-based resonators and oscillators are now coming to the market (see, for instance, [1] and [2]) with applications for RF filtering [3]–[5], frequency references [6], [7], as well as sensing applications [8]–[10]. A common problem encountered by MEMS-based resonators is the need for very precise control of the resonance frequency, both from a manufacturing standpoint (e.g., on-wafer and wafer-to-wafer uniformity) and from a stability perspective (e.g., temperature dependence, aging, and contamination build-up). The resonance frequencies of plates or membranes (e.g., micromirrors or micromachined suspended proof masses) are typically fixed and depend only on geometry and material characteristics (density, Young's modulus, stress, and stress gradients). The need for active tuning of the resonance frequency of silicon beams and plates led to a number of developments [11]–[15] mostly by using comb drives to compress Si beams or to put the beams under tension, or to modify the effective spring constant by addition of an electrostatic force. These techniques are very effective but require large external actuators, typically much larger than the resonator whose frequency one seeks to control.

We present in this paper a resonant device that incorporates the tuning element as part of its structure. The resonating membrane discussed here consists of an electrostatic electroactive polymer (EAP), which is an elastomer sandwiched between two compliant electrodes. The tuning principle is to apply a voltage across the membrane, thus adding compressive stress due to the electrostatic force, hence effectively softening the device and reducing the resonance frequency.

Dielectric EAPs (DEAPs), often referred to as artificial muscles for macroscale actuators, are well known for their exceptional force–displacements characteristics compared to other types of actuators [17]–[20]. Unlike for more conventional materials for microfabrication such as silicon or SiN, we show how the resonance frequency of a prestressed DEAP membrane can be actively tuned after fabrication by changing its internal stress with an applied voltage and associated electrostatic pressure from the compliant electrodes on the surfaces of the elastomer.

While a number of authors have reported on DEAP actuators such diaphragms and membrane rolls [17]–[24], the resonance modes of actuated prestressed DEAP membrane have not yet been reported. We have used polydimethylsiloxane (PDMS) as the elastomer which, combined with standard micromachining processing, allows short response times and resonance frequencies in the audible range (400 Hz–5 kHz).

The working principle of a DEAP is based on the compression of a dielectric elastomer membrane by the electrostatic pressure of compliant electrodes placed on both sides of the membrane (Fig. 1) [17], [18]. The volume of the elastomer being constant (Poisson ratio of 0.5) for free boundary condition, the compression of the elastomer results in an elongation of the elastomer [19]. Depending on the boundary conditions (i.e., what the membrane is bonded to), on the material properties of the membrane and on internal stress, the membrane either buckles, bends, elongates in-plane, or does not move [20]. A number of actuators have been fabricated based on this concept, usually using prestretched films [17]. Since compliant electrodes are required, electrodes for macroscale devices are generally made from carbon powders or silicon greases doped with conductive powders. A major challenge to scaling down

Manuscript received August 13, 2007; revised February 7, 2008. First published July 25, 2008; current version published October 1, 2008. This work was supported in part by the Swiss National Science Foundation under Grant 20021-111841 and in part by the Ecole Polytechnique Fédérale de Lausanne (EPFL). Subject Editor S. Lucyszyn.

P. Dubois, S. Rosset, M. Niklaus, and H. Shea are with the Microsystems for Space Technologies Laboratory, Ecole Polytechnique Fédérale de Lausanne, 1015 Lausanne, Switzerland (e-mail: philippe.dubois@unine.ch).

M. Dadras is with the Institute of Microtechnology, University of Neuchâtel, 2000 Neuchâtel, Switzerland.

Color versions of one or more of the figures in this paper are available online at http://ieeexplore.ieee.org.

Digital Object Identifier 10.1109/JMEMS.2008.927741

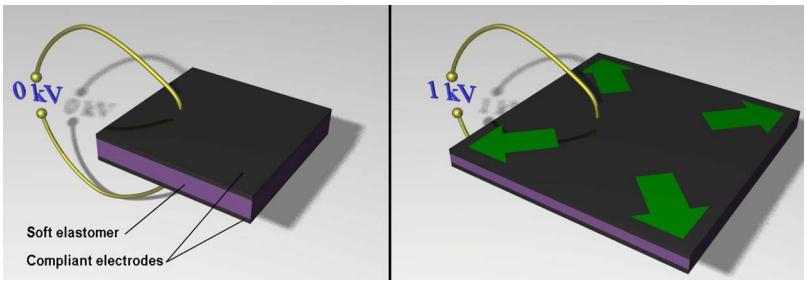

Fig. 1. DEAP principle [25]. When a voltage is applied to the electrodes (typically over 1 kV), the electrostatic pressure squeezes the elastomer dielectric (right side). The volume of the dielectric being quasi-constant, the whole structure stretches in the case of free boundary conditions.

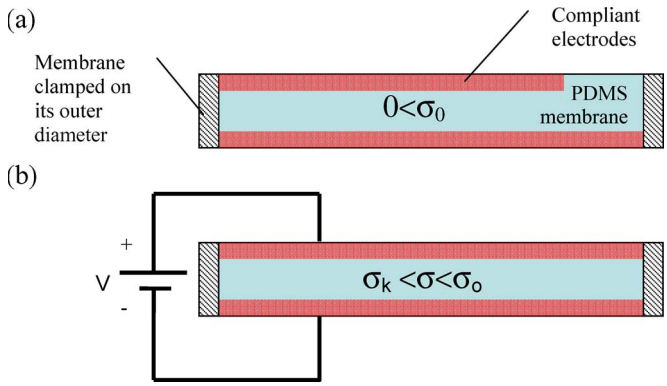

Fig. 2. In-plane stress state in a prestressed membrane. (a) Nonactuated membrane with initial in-plane tensile stress $\sigma_0 > 0$ and (b) actuated membrane with total stress σ, σ_k (with $\sigma_k < 0$) being the buckling critical stress.

these promising actuators to the microscale has been the difficulty of patterning compliant electrodes on the microscale. Since simply sputtering or evaporating metals produces electrodes that are much stiffer than the elastomer [25], a number of approaches have been followed to increase the compliance of microfabricated electrodes (see, for example, the work of Pimpin *et al.* [24]). We have developed an ion implantation technique that allows patterning compliant electrodes in the surface of elastomer membranes [25]–[28].

In this paper, we report on PDMS membranes whose fundamental resonance frequency (a few kilohertz) is tuned by changing its inner stress by means of an electrostatic force (Fig. 2). The modification of the inner stress of the membrane induces a change in the mechanical compliance of the membrane, which can be observed by a change of its resonance frequency.

Although most research and development on MEMS-based resonators is based on silicon devices, there is increasing interest in using polymers such as SU8, polymethyl methacrylate (PMMA), or polyimide as the structural material for MEMS resonators in view of their potential for low cost, simple processing, and higher flexibility. For example, Zhang *et al.* [14], [15] have demonstrated polymer microresonators operating at above 1 MHz.

PDMS is a very soft elastomer, with a Young's modulus on the order of 1 MPa. The devices we report here made with PDMS have a resonant frequency that can be reduced by up to 77% from initial frequencies in the kilohertz range. The same frequency tuning concept could also be used on stiffer resonators that work at much higher frequencies, for instance, for the fine-tuning of resonators that present a resonance frequency

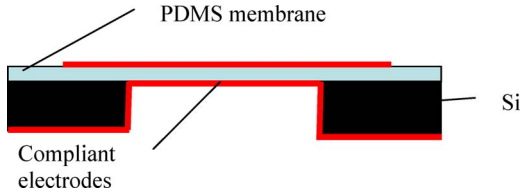

Fig. 3. Schematic cross section of the EAP actuators/membrane showing the location of the implanted/sputtered electrodes.

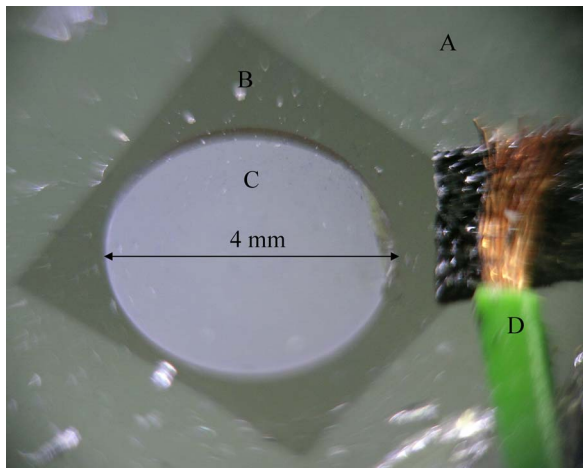

Fig. 4. Photograph of a microfabricated electroactive tunable resonance frequency membrane. The 4-mm-diameter orifice is covered by a PDMS membrane that was implanted on both sides with gold ions at 5 keV with a dose of about 2×10^{16} ions/cm^2. A: PDMS-bonded area. B: Implanted area. C: Free-standing PDMS membrane. D: Top-side electrical connection.

distribution due to process fabrication. Applying our model to the 2-MHz Baytron P-PMMA microbridges of [14], we predict a possible 11.5% tuning range at the electrical breakdown field (PMMA electrical strength: 250 MV/m [16]) or, for example, 1% at 50 V, which is more than sufficient in most cases for fine-tuning drift due to temperature or fabrication variation.

The dielectric electroactive actuator (DEA) studied here consists of a DEAP circular membrane fixed to a rigid Si frame on its outer diameter (Figs. 3 and 4). The membrane is a PDMS film with compliant electrodes on both sides. The fabrication process of the PDMS membrane induces a tensile stress that, along with membrane geometry, membrane density, and Young's modulus, determines the initial resonance frequency. Our membranes are prestressed by the fabrication process, not by mechanically stretching the film prior to bonding to frame (as would be more common for macroscale EAPs).

We have compared two techniques of electrode fabrication that are compatible with small-size electrode patterning: low-energy metal ion implantation and sputtering of metals [25]. We have shown on a proof-of-concept device that metal ion implantation allows the creation of very compliant electrodes that allow for vertical displacement of more than 10% of the membrane's length [25], [26]. The combination of large ion doses ($> 10^{16}$ ions/cm^2) and low energy (< 5 keV), essential to make the elastomer sufficiently conductive, requires the use of special implantation techniques such as plasma immersion ion implantation or filtered cathodic vacuum arc (FCVA). We used our custom FCVA implanting machine to process the samples reported here.

II. Concept and Model

The basic concept is that the resonance frequency $f_{\rm res}$ of membranes under tensile stress can be reduced by reducing the stress. For prestressed DEAP membranes, the initial stress can be reduced by adding an electrostatic stress (Fig. 2) from the applied voltage [see (15)].

Timoshenko [30] derived the resonance frequency of plates in the bending case (zero stress case, where the flexural rigidity dictates $f_{\rm res}$) and of tensile stressed membranes or drums (only stress contribution, no bending dependence, the stress dictates $f_{\rm res}$). We extend their formalism to the more realistic intermediate case of membranes of finite thickness, using the Rayleigh–Ritz approximation to combine the contribution from the bending and stretching energies.

The key assumption we make is that the mode shape is the same for both contributions, which is a reasonable approximation in our case since, as is shown in the data section, the displacement due to the acoustic wave is at most 2% of the membrane diameter.

The Rayleigh–Ritz method allows accurate estimations of the resonance frequency of compliant systems. The membrane starts in the x, y plane. One chooses a trial function $z(x, y, t)$ of the membrane deflection, which, for sinusoidal excitation, can be written as a function of the pulsation ω and time t

$$z(x, y, t) = z(x, y)\cos(\omega t). \tag{1}$$

To determine the resonance pulsation ω_0, we make use of the fact that, at resonance, the maximum kinetic energy $E_{\max}$ and maximum potential (elastic) energy $U_{\max}$ are equal for linear second-order systems. Kinetic energy is maximum when the membrane is flat (minimum membrane deflection), and elastic energy is maximum when velocity is zero (maximum deflection).

As derived in [29], the kinetic energy can be expressed as a function of the density ρ

$$E_{\max} = \frac{\omega^2}{2} \int\limits_{\rm volume} \rho(x, y) \cdot [z(x, y)]^2 \, d{\rm Vol}. \tag{2}$$

The deformation energy $U_{\max}$ can be written as the sum of bending (referred to as plate) and stretching (drum) contributions

$$U_{\max} = U_{\rm plate,max} + U_{\rm drum,max}. \tag{3}$$

Combining (2) and (3) with $E_{\max} = U_{\max}$ gives an expression for the resonance frequency $f_{\rm res} = \omega_{\rm res}/(2\pi)$

$$\omega_{\rm res}^2 = 2\frac{U_{\rm plate,max} + U_{\rm drum,max}}{\int\limits_{\rm volume} \rho(x, y) \cdot [z(x, y)]^2 \, d{\rm Vol}}. \tag{4}$$

With the key approximation of equal mode shapes for plate and drum, this can be written as [see (5)–(9)]

$$\omega_{\rm res}^2 = \omega_{\rm plate}^2 + \omega_{\rm drum}^2 \tag{5}$$

where the plate pulsation $\omega_{\rm plate}$ can be expressed as a function of the membrane diameter d, thickness h, membrane homogenous density ρ, and flexural rigidity D [30], [31]

$$\omega_{\rm plate}^2 = 2\frac{U_{\rm plate,max}}{\int\limits_{\rm volume} \rho(x, y) \cdot [z(x, y)]^2 \, d{\rm Vol}} = \left(\frac{40.704}{d^2}\right)^2 \frac{D}{\rho h} \tag{6}$$

with the flexural rigidity D that depends on the Young's modulus Y and Poisson's ratio ν, which is given by

$$D = \frac{Y h^3}{12(1 - \nu^2)}. \tag{7}$$

The drum pulsation $\omega_{\rm drum}$ as a function of the stress $\sigma_{x,y}$ and diameter d is given by [30], [31]

$$\begin{aligned}\omega_{\rm drum}^2 &= 2\frac{U_{\rm drum,max}}{\int\limits_{\rm volume} \rho(x, y) \cdot [z(x, y)]^2 \, d{\rm Vol}} \\ &= \left(\frac{4.81}{d}\right)^2 \frac{\sigma_{x,y}}{\rho}, \qquad \text{valid for } \sigma_{x,y} \geq 0.\end{aligned} \tag{8}$$

Therefore, we have the resonance frequency f of a stressed membrane that is not perfectly thin, i.e., a plate

$$\begin{aligned} f &= \sqrt{f_{\rm plate}^2 + f_{\rm drum}^2} \\ f &= \frac{1}{2\pi d\sqrt{\rho}} \sqrt{23.13\sigma_{x,y} + \frac{1657}{d^2}\frac{D}{h}}, \\ &\qquad \text{valid for } \sigma_{x,y} \geq 0. \end{aligned} \tag{9}$$

The initial stress state in a biaxially uniformly tensile stressed membrane is defined as follows:

$$\sigma_{0x} = \sigma_{0y} = \sigma_0 > 0 \tag{10}$$

$$\sigma_{0Z} \cong 0. \tag{11}$$

Assuming that there is no displacement of the membrane (no buckling or bending, which is realistic below the buckling threshold), the stress produced by the electrostatic force is hydrostatic, i.e., there are only identical terms in the diagonal

of the stress tensor $[\sigma_E]$ [32]. The total stress is the sum of the initial stress $[\sigma_0]$ and the electrostatic stress $[\sigma_E]$

$$[\sigma] = [\sigma_0] + [\sigma_E] \tag{12}$$

$$[\sigma] = \begin{bmatrix} \sigma_0 & 0 & 0 \\ 0 & \sigma_0 & 0 \\ 0 & 0 & 0 \end{bmatrix} + \begin{bmatrix} \sigma_E & 0 & 0 \\ 0 & \sigma_E & 0 \\ 0 & 0 & \sigma_E \end{bmatrix} = \begin{bmatrix} \sigma_0 + \sigma_E & 0 & 0 \\ 0 & \sigma_0 + \sigma_E & 0 \\ 0 & 0 & \sigma_E \end{bmatrix} \tag{13}$$

with the electrostatic stress produced by the actuation voltage V given by

$$\sigma_z = \sigma_E = -\varepsilon \frac{V^2}{h^2} \tag{14}$$

with ε as the permittivity of the elastomer.Therefore, according to (13), the stress in the plane x, y when the membrane is actuated becomes

$$\sigma_x = \sigma_y = \sigma_0 - \varepsilon \frac{V^2}{h^2}. \tag{15}$$

Equations (8) and (9) are only strictly valid for $\sigma_{x,y} \geq 0$. Chen and Doong [33] have developed a more complex model for thick plates in which they extend the calculation of the resonance frequency to the compressive regime.

Combining (9) with (15), we obtain the first mode resonance frequency of an actuated circular membrane as

$$f = \frac{1}{2\pi d\sqrt{\rho}} \sqrt{23.13\left(\sigma_0 - \frac{\varepsilon}{h^2} V^2\right) + \frac{1657}{d^2} \frac{D}{h}}. \tag{16}$$

From (16), one sees that the resonance frequency can be tuned down from its initial value by applying a voltage on the electrodes. According to this model, the membrane resonance frequency can be voltage tuned from f_{high} to $f_{\text{no\_stress}}$

$$f_{\text{no\_stress}} \leq f_{\text{actuated}} \leq f_{\text{high}} \tag{17}$$

$$\text{With : } f_{\text{high}} = \frac{1}{2\pi d\sqrt{\rho}} \sqrt{23.13\sigma_0 + \frac{138.1}{d^2} \frac{Yh^2}{1-\nu^2}} \tag{18}$$

$$f_{\text{no\_stress}} = \frac{1}{2\pi d\sqrt{\rho}} \sqrt{\frac{138.1}{d^2} \frac{Yh^2}{1-\nu^2}}. \tag{19}$$

The higher the initial stress is, the higher the frequency span becomes. However, in practice, resonance frequencies below $f_{\text{no\_stress}}$ corresponding to compressive stresses below the buckling threshold can also be reached as described by Chen and Doong [33].

For typical DEAP membrane parameters, Fig. 5 compares the model given by (16) with the model of Chen and Doong for thick plates [33] applied to the DEAP stress situation, i.e., substitution of the in-plane stress used in the model of Chen and Doong with the total stress of (15). The two curves agree within 7% in the tensile domain, the largest discrepancy of 168 Hz being found when the membrane is not actuated. As discussed in the data section, the model presented here based on Rayleigh–Ritz theory gives a better fit of the measured data in the tensile region than the model based on Chen and Doong for thick plates [33].

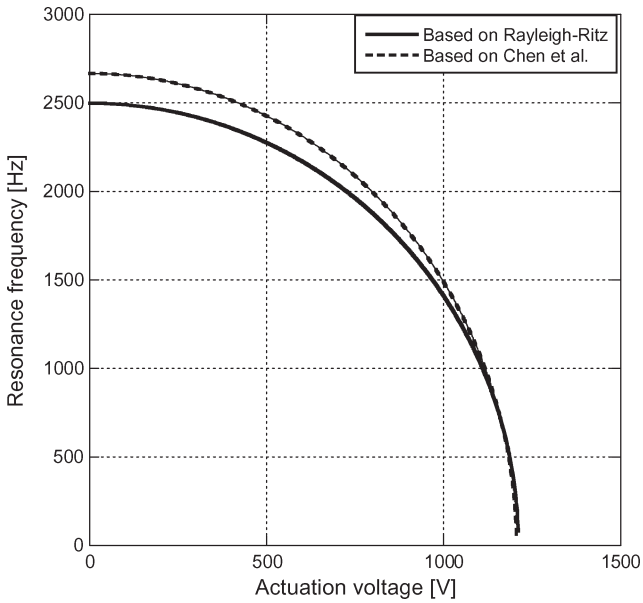

Fig. 5. Comparison between two models of the resonance frequency versus applied voltage for DEAP membranes. The (solid line) first model is based on Rayleigh–Ritz theory [see (16)], and the (dashed line) second model is the one of Chen and Doong [33] applied to the DEAP with tensile stress situation. We used the following typical parameters: $Y = 1$ MPa, $\sigma_0 = 50$ kPa, $h = 28.6$ μm, $d = 2$ mm, and $\nu = 0.5$.

For low stresses and high actuation voltages, the models also agree remarkably well even in the regime where the film is in compression, beyond the normal domain of applicability of our model. For geometry and material properties similar to the one described in Fig. 5, we found that the stress buckling condition based on our modeling [see (20) and (21)] is 13% higher than the one computed with the model of Chen and Doong [33] and 22% higher than the one based on standard plate buckling threshold [28]. Also, the buckling voltage given by the Rayleigh–Ritz model [see (22)] matches the one from the model of Chen and Doong [33] and standard plate theory [28] to better than one 1%. Therefore, the domain of applicability of our model based on Rayleigh–Ritz theory can be extended to the compressive domain of a DEAP membrane

$$0 = 23.13\left(\sigma_0 - \frac{\varepsilon}{h^2} V_k^2\right) + \frac{1657}{d^2} \frac{D}{h}, \quad \text{buckling condition} \tag{20}$$

$$\sigma_k = -71.62 \frac{D}{d^2 h} \tag{21}$$

$$V_k = h\sqrt{\frac{\sigma_0 - \sigma_k}{\varepsilon}} = \sqrt{\frac{h}{\varepsilon}\left(23.13\sigma_0 h + \frac{1657D}{d^2}\right)}. \tag{22}$$

The electrical breakdown of the elastomer typically occurs before the initial stress can be completely compensated, thus increasing the minimum achievable resonance frequency. Also, for the model, we assumed a circular membrane considered homogenous along its thickness, i.e., any localized stiffening due to the electrodes on the surface is ignored.

III. Fabrication and Design

A. Fabrication Process

The samples consist of an electroactive silicone membrane bonded over a circular orifice etched through a 500-μm-thick silicon wafer (Fig. 4). We developed a microfabrication process to pattern the compliant electrodes, produce the membrane, and bond the membrane to the silicon. Most of the fabrication developments concerned an ion implantation technique used to produce compliant electrodes on the EAP. To have a high-performance EAP device, it is necessary to have compliant electrodes that can repeatedly sustain strains of over 10% and that do not overly stiffen the membrane, i.e., that the stiffness of the two electrodes be smaller than the stiffness of the elastomer. This last point is not trivial given that metals have a Young's modulus four orders of magnitude larger than the elastomers we use. Ion implantation of gold gave excellent electrodes that can be patterned on the micrometer scale. Suitable micropatterning of the electrodes is also a possibility [24].

Circular holes, 2–4 mm in diameter, were patterned by deep reactive ion etching in 4-in silicon wafers. The PDMS layer was spun on a transfer support, a polyvinylidene chloride (PVDC) film stressed on a rigid frame. Once the PDMS (Dow Corning Sylgard 186) polymerized, the PDMS membrane was bonded after plasma O_2 treatment on the silicon chip and detached from its PVDC supporting film [25].

Metal ion implantation was carried out in an experimental setup which is capable of implanting only a zone of a few square centimeters, thus explaining the need of a chip-level process rather than a wafer-level one. However, the steps described earlier to obtain a thin membrane bonded on Si have also been successfully tested on the entire 4-in Si wafers.

Our custom FCVA implantation equipment is based on a commercial pulsed arc ion source (ARC 20 RHK). Topside implantation is carried out through a steel shadow mask, but a photoresist mask patterned by photolithography could also be used on a wafer-scale process. Backside implantation is done without masks, through the orifice in the silicon chip. Gold ions are deposited on the back of the membrane, but also on the edge of the Si chip, thus ensuring electrical contact between the membrane and the silicon chip, which can act as a contact to one electrode during actuation (Fig. 3). The gold ion implantation parameters are a dose of $1.7-2*10^{16}$ atoms/cm^2 as determined by RBS, initial acceleration energy of 5 kV at each pulse (the bias decreases during each implantation pulse and is restored before the next pulse).

Cathodic sputtering (SCD030 Balzers) of gold layers between 8 and 15 nm thick has also been tested to compare the impact of this method versus implantation on the resonance frequency of the membranes.

B. Control of Initial Resonance Frequency

The initial (nonactuated) resonance frequency of a membrane is essentially defined by the following parameters:

1) geometry of the membrane;
2) boundary conditions;
3) PDMS mechanical properties;
4) influence of the electrodes.

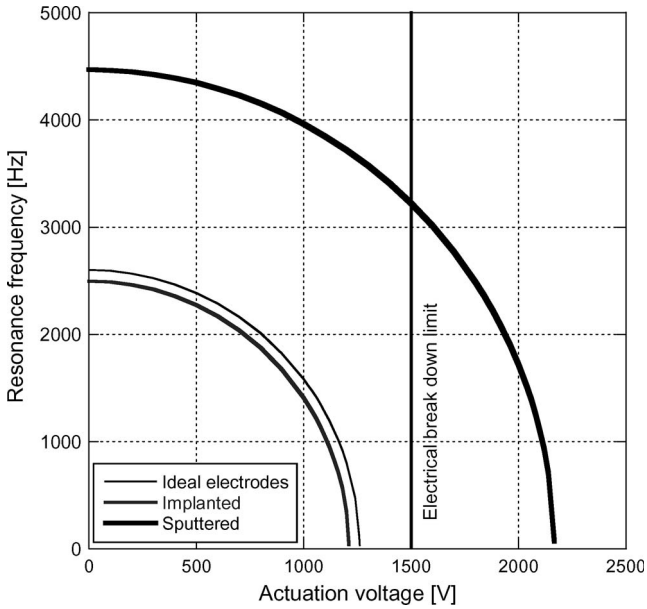

Fig. 6. Simulated resonance frequency versus applied voltage to illustrate the influence of the stiffening of the membrane due to the electrodes. Ideal electrodes do not stiffen the membrane. The plots are generated using typical parameters measured on a 2-mm-diameter 28.6-μm-thick membrane. Bare PDMS ($Y = 1$ MPa, $\sigma_0 = 50$ kPa), ion-implanted PDMS ($Y = 2.6$ MPa, $\sigma_0 = 43.4$ kPa), and sputtered PDMS ($Y = 7$ MPa, $\sigma_0 = 141$ kPa).

1) Influence of Membrane Geometry: The geometry of the membrane in the plane is very well controlled by the microfabrication process, i.e., tolerance on the membrane diameter of ± 2 μm.

Variations of the membrane thickness h up to ± 2 μm were observed with an optical white light profilometer (Veeco, Wyco NT1100). Due to instrument limitations, the thickness measurements were done on the PDMS bonded to the Si, not on the free-standing membrane. We were not able to make a distinction between real variations and measurement errors. Thickness variations have a significant impact on the resonance frequency, particularly at high actuation voltages.

2) Influence of Boundary Conditions: In our fabrication process, the PDMS membrane is bonded on silicon; hence, the membrane is fixed only on the bottom part. The membrane having a diameter-to-thickness ratio larger than 50, the membrane is quasi-perfectly fixed and can be considered clamped on its edge.

3) Influence of PDMS Mechanical Properties: The Young's modulus of different PDMS formulations varies by a factor of more than ten. In addition, both Young's modulus and stress can be controlled over a limited range by modifying the process parameters [25]. We observed that the internal stress is highly dependent on the PDMS curing temperature. As a rule of thumb, the higher the curing temperature, the higher the stress. Therefore, by tuning the temperature and stress, it is possible to meet specific requirements concerning the resonance frequency domain of interest. The tensile stress has a major impact on the membrane initial resonance frequency f_{high}.

4) Influence of Electrode Type: Fig. 6 shows, based on the analytical model [see (16)], the effect of electrode compliance on the frequency span for three different electrode types: ideally

compliant (causing no additional stiffening), ion implanted, and sputtered electrodes. The sputtered electrodes consist of metal deposited on top of the PDMS membrane. The implanted electrodes have metal ions buried within the PDMS. The parameters Y and σ_0 are typical average values measured by bulge test [25], [34], [35] on 2-mm-diameter Sylgard 186 membranes. Electrical fields larger than 50 V/μm are larger than the typical breakdown field for commercially available PDMS.

Sputtered gold electrodes significantly stiffen the membrane, increasing the overall Young's modulus Y (by a factor of 5 to over 20 depending on deposition conditions) and the residual stress σ_0 (about a factor of 2–3). This pushes the frequency versus actuation voltage curve toward higher frequencies. The thickness of very thin sputtered layers ($<$ 20 nm), required by this application, is difficult to control and has a major impact on the overall membrane properties. Based on (16), the influence of the stress σ_0 and Young's modulus Y can be estimated by the model (Fig. 6). The large stress increase coming from sputtering produces a strong curve displacement upward that is not well controlled and difficult to take into account in the design.

Ion implantation of metallic ions into the polymer minimizes the electrodes' impact on the mechanical properties of the membrane (Fig. 6). For ion-implanted gold, we observed an increase of the overall Young's modulus due to ion implantation of about a factor of 1.5–3 and a limited modification of the inner overall stress of $\pm 20\%$ on most samples toward a reduction, which is the case in Fig. 6. Such a limited modification of the stress enables one to design an actuator with well-defined initial resonance frequency. The limited modification of the Young's modulus favors a low frequency that can be reached when the actuator is fully actuated.

IV. Resonance Frequency Characterization

A. Testing Setup

We introduced in the model developed on Rayleigh–Ritz theory [see (16)] the average parameters (Y, σ_0) measured by bulge test and profilometer (Veeco, Wyco NT1100) after electrode fabrication. To take into account the stiffening due to the electrodes, we used a standard bulge test technique applied on the actuator membrane having its electrodes already fabricated. To extract the parameters (Y, σ_0), the data points were fitted with the bulge test equation [25], [34], [35]

$$p = (1 - 0.24\nu)\frac{8Y}{3 - 3\nu}\frac{h}{r^4}z^3 + 4\frac{\sigma_0 h}{r^2}z \qquad (23)$$

where r is the membrane radius, p is the applied pressure, and z is the vertical deflection of the membrane's center. To measure the membrane thickness h, a scratch was made on each sample in an area of the PDMS bonded to the silicon chip, and the step height was measured with the same profilometer.

The resonance frequency of PDMS membranes was measured by applying a sound wave with a loudspeaker on one side of the membrane and measuring the membrane displacement with a laser Doppler vibrometer (Polytec MSV400, Fig. 7). These measurements were done with an actuation voltage ranging from 0 to 1.8 kV.

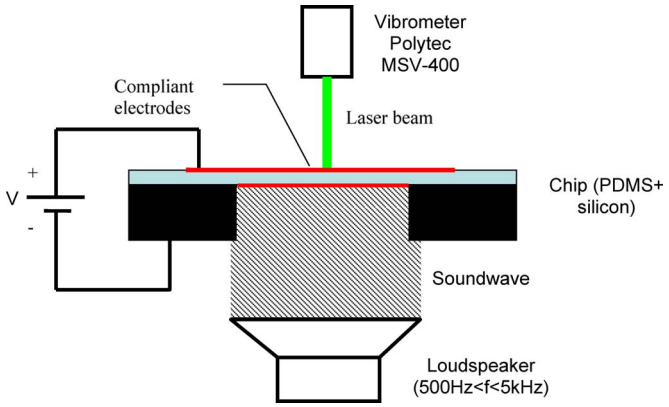

Fig. 7. Schematic of the resonance frequency measurement setup combining acoustic excitation and electrostatic actuation.

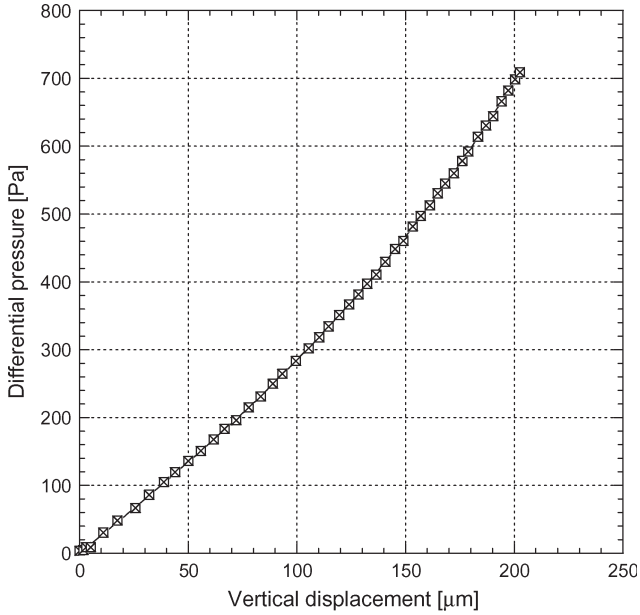

Fig. 8. Bulge-test measurements realized with a profilometer (Veeco, Wyco NT1100) of the 4-mm-diameter membrane made in PDMS Sylgard 184. The differential gas pressure applied on the membrane is plotted as a function of the membrane vertical displacement. The data points, fitted with bulge-test equation using the membrane thickness measured with the same profilometer ($h = 35$ μm), result in a Young's modulus of 2.04 MPa and a tensile stress of 75.42 kPa.

Displacement of the center of the membrane was measured while the drive frequency was swept in order to find the resonances. Mode shapes were then determined by scanning the laser at a fixed drive frequency.

B. Results

To apply the frequency model, the membrane mechanical properties (Y, σ_0) were measured with the bulge test setup. We recorded the applied gas pressure versus displacement of each membrane and fitted the data points with the bulge test equation [25] (Fig. 8). The parameters of the tested samples used for calculation in the model are summarized in Table I.

The first mode shape was recorded on a 4-mm-diameter membrane made in Sylgard 184 at 0–1500-V actuation voltage

TABLE I
SUMMARY OF THE PARAMETERS USED IN THE MODEL AND THE CALCULATED RESONANCE FREQUENCIES. THE MEASURED INITIAL RESONANCES ARE ALSO GIVEN FOR COMPARISON. YOUNG'S MODULUS AND INITIAL STRESS ARE MEASURED BY BULGE TEST, MEMBRANE THICKNESS IS MEASURED WITH AN OPTICAL PROFILOMETER, AND OTHER PROPERTIES OF THE SYLGARD 184 AND 186 PDMS FROM DOW CORNING ARE THE ONES PROVIDED BY THE MANUFACTURER

	Implanted d = 4 mm Sylgard 184	Implanted d = 2 mm Sylgard 186	Sputtered d = 2 mm Sylgard 186
Diameter d [mm]	4	2	2
Measured thickness h [µm]	35	28.6	20.4
Density ρ [kg/m^3] [Dow Corning]	1050	1120	1120
Relative dielectric permittivity ε	3	3	3
Measured average Young's modulus Y [MPa]	2.04	2.6	7.54
Measured average initial stress σ_0 [kPa]	75.42	43.4	140.94
Calculated initial resonant frequency in mode 1 f_{high} [Hz]	1636	2496	4387
Measured initial resonant frequency in mode 1 f_{high} [Hz]	1620	2463	4450

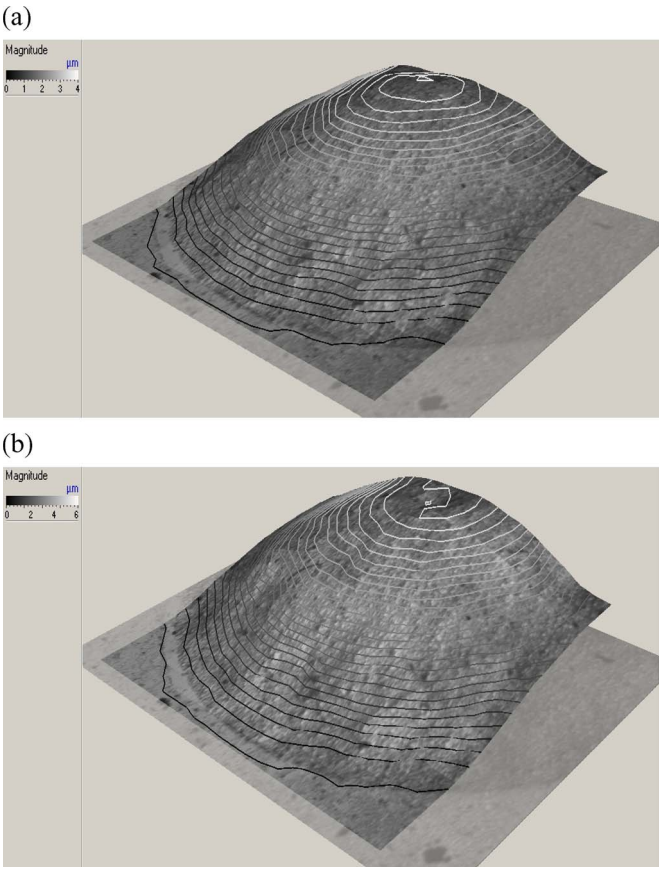

Fig. 9. Measured mode shapes of the 4-mm-diameter membrane made in PDMS Sylgard 184: (a) not actuated ($f_{\rm res} = 1620$ Hz) and (b) actuated at 1500 V ($f_{\rm res} = 975$ Hz).

(Fig. 9). Although the maximum amplitude does increase with the applied voltage (since the membrane becomes more compliant as the initial stress is canceled by the applied electrostatic

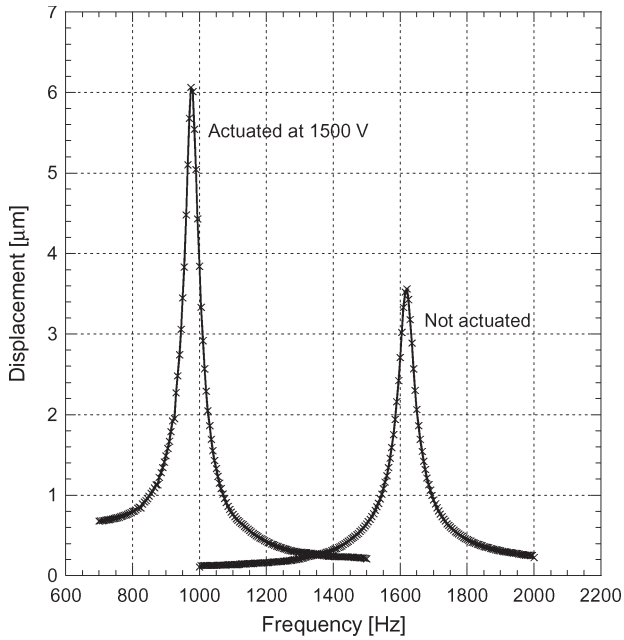

Fig. 10. Measured resonance peaks of the 4-mm-diameter membrane made in PDMS Sylgard 184: (a) not actuated ($f_{\rm res} = 1620$ Hz, $Q = 20$) and (b) actuated at 1500 V ($f_{\rm res} = 975$ Hz, $Q = 15$).

stress), the shape of mode 1 remains the same from 0 to 1.5 kV as the $f_{\rm res}$ decreases.

We measured typical quality factors of $Q = 45$ on a 3-mm-diameter Sylgard 186 membrane and $Q = 20$ on a 4-mm-diameter Sylgard 184 membrane (Fig. 10). The quality factor tends to decrease when the membrane is actuated. This effect is limited to a few percents at low actuation voltages and becomes significant when the resonance frequency is strongly reduced: A factor 2 reduction of Q is observed for 1800-V actuation voltage on the 4-mm-diameter Sylgard 184 membrane.

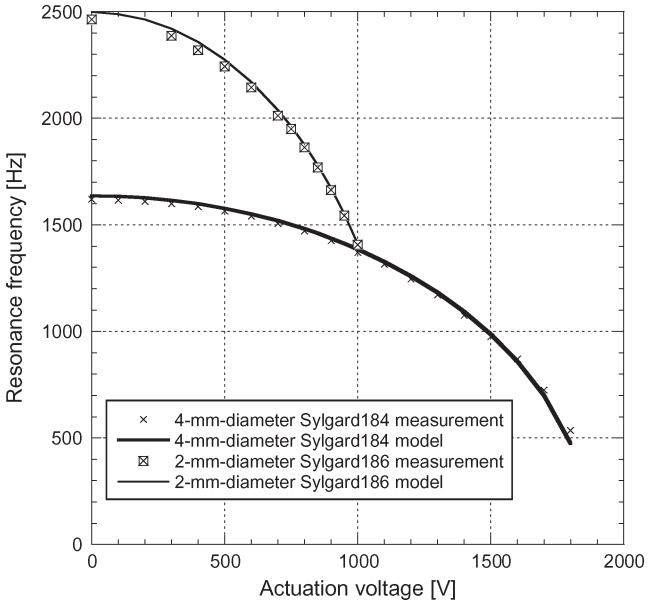

Fig. 11. Resonance frequency as a function of actuation voltage for two gold ion-implanted membranes. Sample A is a 2-mm-diameter membrane made of PDMS Sylgard 186. Sample B is a 4-mm-diameter membrane made from Sylgard 184. The squares and "x"'s correspond to measurements on samples A and B, respectively, and the solid lines are computed from the model of (16) (no free parameters for the fit, parameters obtained from the bulge test and profilometer data are for sample A: $Y = 2.6$ MPa, $\sigma_0 = 43.4$ kPa, and $h = 28.6$ μm, and for sample B: $Y = 2.04$ MPa, $\sigma_0 = 75.42$ kPa, and $h = 35$ μm).

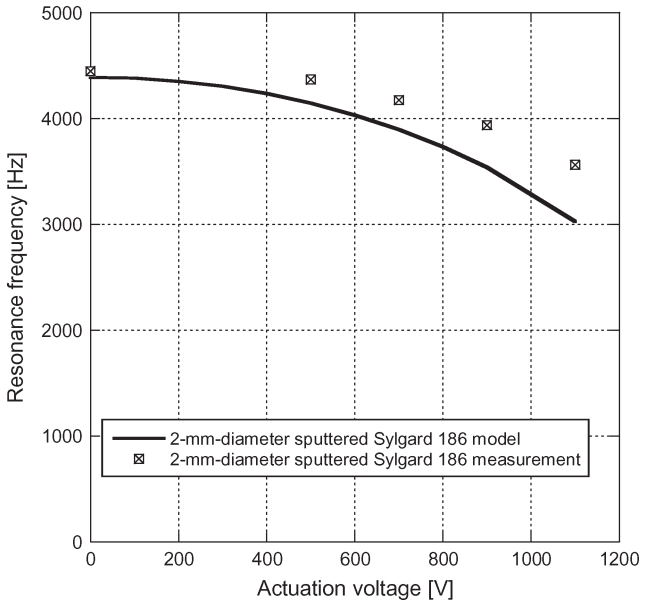

Fig. 12. Resonance frequency as a function of actuation voltage for a 2-mm-diameter membrane having sputtered electrodes (PDMS Sylgard 186). The measurement is compared to the model ($Y = 7$ MPa, $\sigma_0 = 141$ kPa, and $h = 20.4$ μm). The sputtered electrodes significantly stiffen the membrane, increasing the resonance frequency and reducing the percent tuning range.

For membrane of two diameters and with different physical properties, we observed the predicted shift of the resonance frequency produced by electrostatic actuation. For the Au ion-implanted 2-mm-diameter Sylgard 186 sample actuated at 1000 V (Fig. 11), the relative resonance frequency shift was -43% (from 2463 down to 1406 Hz); for the Au ion-implanted 4-mm-diameter Sylgard 184 sample actuated at 1800 V, the shift was -77%; and for the sputtered 2-mm-diameter Sylgard 186 membrane, the shift was -20% (from 4450 down to 3563 Hz, Fig. 12) at 1100V. Maximum voltages were limited by the need to stay below the dielectric breakdown field.

An excellent match (difference: $< 1.5\%$ nonactuated, $< 10\%$ at full actuation) between the resonance frequency model and measurements on ion-implanted samples was observed (Fig. 11). Also, if the model of Chen and Doong is used to fit the data points, a larger discrepancy, for instance 8% for the 2-mm-diameter implanted sample, is observed at high resonance frequency and low actuation voltage.

On sputtered samples (Fig. 12), the larger observed discrepancy between model and data at high actuation voltages could be due to the fact that the model takes into consideration only average input parameters, i.e., no gradients of Young's modulus and stress are considered in the composite created by the electrodes.

Also, one should mention that the accurate measurement of the membrane thickness is very critical since this parameter has a large impact on the calculated frequencies, particularly when actuated at high voltages.

One can rewrite (16) as (24) in order to make clearer that, in the resonance frequency model, f^2 scales with V^2

$$f^2 = \frac{1}{(2\pi d)^2 \rho}\left(23.13\sigma_0 + \frac{1657 Y h^2}{12(1-\nu^2)d^2} - 23.13\frac{\varepsilon}{h^2}V^2\right). \tag{24}$$

Therefore, by fitting f^2 to V^2, one can determine the thickness if the relative permittivity, density, and diameter are known. Those three values are easily determined with high precision by other techniques. Therefore, the model can be used to measure indirectly the membrane thickness h'. To refine the membrane properties, the fitted thickness h' can be introduced in the bulge test equation to determine Y' and σ_0' with a better accuracy.

V. Conclusion

Unlike more standard materials used in microfabricated membranes (such as SiN or Si) whose resonance frequency is fixed by geometry and material properties, the resonance frequency of microfabricated dielectric EAP membranes was repeatedly and reversibly voltage controlled, allowing the compliance of the membrane to be tuned continuously over a range up to 77%. Two types of compliant electrodes were tested on the PDMS membranes: thin (10–20 nm) sputtered gold and implanted gold (a dose of 4.4×10^{16} atoms/cm^2). For ion-implanted devices, on the 2-mm-diameter Sylgard 186 membrane, an actuation voltage of 1 kV changed in the resonance frequency of the membrane by more than 40%, whereas on the 4-mm-diameter Sylgard 184 membrane, at 1.8-kV actuation voltage, the change was -77%. Sputtered electrodes that significantly stiffen and stress the membrane have a smaller achievable tuning range that is limited by the PDMS breakdown voltage.

For ion-implanted samples, an analytical model was developed based on the sum of energies from two different contributions, corresponding to stress-dominated thin film, and zero-stress plate. This model gave very good agreement with the measured data when used with membrane parameters entirely obtained from other characterization techniques, primarily bulge testing (no free parameters). The slightly lower accuracy of the model observed for less compliant sputtered electrodes reveals the approximation of the model that does not consider gradients of stress and Young's modulus.

The model that was initially developed to describe the resonance frequency of a DEAP membrane in the tensile stress domain also provides an excellent estimation in the compressive region matching to 1% the buckling voltage resulting from a thick plate model developed by Chen and Doong [33] when applied to the DEAP membrane. To describe the entire range of actuation going from 0 V to the buckling voltage, the model based on Rayleigh–Ritz theory provides the best approximation.

Verifications of the first mode shape and quality factor show that they are not significantly modified when the resonance frequency is shifted. The work reported here on PDMS can be extended to any dielectric elastomer, such as acrylic commonly used in EAP actuators, and also to polymers more commonly used in microfabrication. A similar modeling approach could certainly allow the derivation of a theory describing the higher order resonance modes.

The ability to tune resonance frequency and compliance of a membrane could find applications in active filters, analog sound processing, and active damping for devices resonating in the kilohertz range, and as fine-tuning of resonance frequency of megahertz resonators used as frequency references, RF filters, and sensors.

ACKNOWLEDGMENT

The authors would like to thank the COMLAB staff for helping with the device fabrication.

REFERENCES

[1] SiTime Corporation. [Online]. Available: www.sitime.com
[2] Discera Inc. [Online]. Available: www.discera.com
[3] G. Piazza, P. J. Stephanou, and A. P. Pisano, "Single-chip multiple-frequency ALN MEMS filters based on contour-mode piezoelectric resonators," *J. Microelectromech. Syst.*, vol. 16, no. 2, pp. 319–328, Apr. 2007.
[4] Y.-W. Lin, S.-S. Li, Z. Ren, and C. T.-C. Nguyen, "Vibrating micromechanical resonators with solid dielectric capacitive-transducer 'gaps'," in *Proc. Joint IEEE Int. Freq. Control/Precision Time Interval Symp.*, Vancouver, BC, Canada, Aug. 29–31, 2005, pp. 128–134.
[5] R. Melamud, B. Kim, S. Chandorkar, M. Hopcroft, M. Agarwal, C. Jha, and T. W. Kenny, "Temperature compensated high-stability silicon resonators," *Appl. Phys. Lett.*, vol. 90, no. 24, p. 244 107, Jun. 2007.
[6] C. Nguyen, "MEMS technology for timing and frequency control," *IEEE Trans. Ultrason., Ferroelectr., Freq. Control*, vol. 54, no. 2, pp. 251–270, Feb. 2007.
[7] Y. Lin, S. Lee, S. Li, Y. Xie, Z. Ren, and C. Nguyen, "Series-resonant VHF micromechanical resonator reference oscillators," *IEEE J. Solid-State Circuits*, vol. 39, no. 12, pp. 2477–2491, Dec. 2004.
[8] K. L. Ekinci, X. M. H. Huang, and M. L. Roukes, "Ultrasensitive nanoelectromechanical mass detection," *Appl. Phys. Lett.*, vol. 84, no. 22, pp. 4469–4471, May 2004.
[9] K. L. Ekinci and M. L. Roukes, "Nanoelectromechancial systems," *Rev. Sci. Instrum.*, vol. 76, no. 6, p. 061 101, Jun. 2005.
[10] N. V. Sepaniak, M. J. Datskos, and P. G. Lavrik, "Cantilever transducers as a platform for chemical and biological sensors," *Rev. Sci. Instrum.*, vol. 75, no. 7, pp. 2229–2253, Jul. 2004.
[11] S. G. Adams, F. M. Bertsch, K. A. Shaw, P. G. Hartwell, F. C. Moon, and N. C. MacDonald, "Capacitance based tunable resonators," *J. Micromech. Microeng.*, vol. 8, no. 1, pp. 15–23, Mar. 1998.
[12] B. E. DeMartini, J. F. Rhoads, K. L. Turner, S. W. Shaw, and J. Moehlis, "Linear and nonlinear tuning of parametrically excited MEMS oscillators," *J. Microelectromech. Syst.*, vol. 16, no. 2, pp. 310–318, Apr. 2007.
[13] J. I. Seeger and B. E. Boser, "Parallel-plate driven oscillations and resonant pull-in," in *Proc. Solid-State Sensor, Actuator Microsyst. Workshop*, Hilton Head Island, SC, Jun. 2–6, 2002, p. 313.
[14] G. Zhang, J. Gaspar, V. Chu, and J. P. Conde, "Electrostatically actuated polymer microresonators," *Appl. Phys. Lett.*, vol. 87, no. 10, p. 104 104, Sep. 2005.
[15] G. Zhang, V. Chu, and J. P. Conde, "Electrostatically actuated bilayer polyimide-based microresonators," *J. Micromech. Microeng.*, vol. 17, no. 4, pp. 797–803, Apr. 2007.
[16] K. Miyairi and E. Itoh, "AC electrical breakdown and conduction in PMMA thin films and the influence of $LiClO_4$ as an ionic impurity," in *Proc. Int. Conf. Solid Dielectrics*, Toulouse, France, Jul. 5–9, 2004.
[17] S. Ashley, "Artificial muscles," *Sci. Amer.*, vol. 289, no. 4, pp. 52–59, 2003.
[18] Y. Bar-Cohen, "Electro-active polymers: Current capabilities and challenges," in *Proc. SPIE—Smart Structures and Materials: EAPAD*, 2002, vol. 4695, pp. 1–7.
[19] P. Sommer-Larsen, G. Kofod, M. H. Shridhar, M. Benslimane, and P. Gravesen, "Performance of dielectric elastomer actuators and materials," in *Proc. SPIE—Smart Structures and Materials: EAPAD*, 2002, vol. 4695, pp. 158–166.
[20] R. E. Pelrine, R. D. Kornbluh, and J. P. Joseph, "Electrostriction of polymer dielectrics with compliant electrodes as a means of actuation," *Sens. Actuators A, Phys.*, vol. 64, no. 1, pp. 77–85, Jan. 1998.
[21] R. Heydt, R. Kornbluh, R. Pelrine, and V. Mason, "Design and performance of an electrostrictive-polymer film acoustic actuator," *J. Sound Vib.*, vol. 215, no. 2, pp. 297–311, Aug. 1998.
[22] S. P. Lacour, H. Prahlad, R. Pelrine, and S. Wagner, "Mechatronic system of dielectric elastomer actuators addressed by thin film photoconductors on plastic," *Sens. Actuators A, Phys.*, vol. 111, no. 2/3, pp. 288–292, Mar. 2004.
[23] F. Carpi and D. De Rossi, "Dielectric elastomer cylindrical actuators: Electromechanical modelling and experimental evaluation," *Mater. Sci. Eng. C*, vol. 24, no. 4, pp. 555–562, Jun. 2004.
[24] A. Pimpin, Y. Suzuki, and N. Kasagi, "Micro electrostrictive actuator with large out-of-plane deformation for flow-control application," *J. Microelectromech. Syst.*, vol. 16, no. 3, pp. 753–764, Jun. 2007.
[25] S. Rosset, M. Niklaus, P. Dubois, M. Dadras, and H. R. Shea, "Mechanical properties of electroactive polymer microactuators with ion implanted electrodes," in *Proc. SPIE—EAPAD*, Y. Bar-Cohen, Ed., 2007, vol. 6524, p. 10.
[26] P. Dubois, S. Rosset, S. Koster, J. Stauffer, S. Mikhailov, M. Dadras, N.-F. D. Rooij, and H. Shea, "Microactuators based on ion implanted dielectric electroactive polymer (EAP) membranes," *Sens. Actuators A, Phys.*, vol. 130/131, pp. 147–154, Aug. 2006.
[27] S. Rosset, M. Niklaus, P. Dubois, and H. R. Shea, "Performance characterization of miniaturized dielectric elastomers fabricated using metal ions implantation," in *Proc. MEMS*, Tucson, AZ, 2008, pp. 503–506.
[28] S. Rosset, M. Niklaus, P. Dubois, and H. R. Shea, "Mechanical characterization of a dielectric elastomer microactuator with ion-implanted electrodes," *Sens. Actuators A, Phys.*, vol. 144, no. 1, pp. 185–193, May 2008.
[29] S. D. Senturia, *Microsystem Design*. Norwell, MA: Kluwer, 2001.
[30] S. Timoshenko *et al.*, *Vibrations Problems in Engineering*, 4th ed. Hoboken, NJ: Wiley, 1974.
[31] H. Dubbel, *Handbook of Mechanical Engineering*. New York: Springer-Verlag, 1994.
[32] E. Popov, *Introduction to Mechanics of Solids*. Englewood Cliffs, NJ: Prentice-Hall, 1968, p. 319.
[33] L.-W. Chen and J.-L. Doong, "Vibrations of an initially stressed transversely isotropic circular thick plate," *Int. J. Mech. Sci.*, vol. 26, no. 4, pp. 253–263, 1984.
[34] J. J. Vlassak and W. D. Nix, "A new bulge test technique for the determination of Young's modulus and Poisson's ratio of thin films," *J. Mater. Res.*, vol. 7, no. 12, pp. 3242–3249, 1992.
[35] V. Paviot, J. Vlassak, and W. Nix, "Measuring the mechanical properties of thin metal films by means of bulge testing of micromachined windows," in *Proc. Mater. Res. Soc. Symp.*, 1995, vol. 356, pp. 579–584.

Philippe Dubois received the Diploma in electricity/electronics from the University of Applied Sciences, Le Locle, Switzerland, and the Diploma in physics/electronics and the Ph.D. degree in microsystems from the University of Neuchâtel, Neuchâtel, Switzerland.

His domains of interest include silicon- and polymer-based microelectromechanical systems, artificial muscles, ion implantation, nanocomposites, wireless sensor networks, and space exploration. After two years of postdoctoral research on multi-directional accelerometers in the group of Prof. de Rooij, he joined the group of Prof. Shea at the Ecole Polytechnique Fédérale de Lausanne, Lausanne, Switzerland, where he currently leads research on dielectric electroactive elastomer actuators.

Samuel Rosset received the M.Sc. degree in microengineering in 2004 from the Ecole Polytechnique Fédérale de Lausanne (EPFL), Lausanne, Switzerland, where he is currently working toward the Ph.D. degree.

In 2005, he joined the group of Prof. Shea at the EPFL as a Ph.D. student working on small-size DEAs. His current activities involve the characterization of ion-implanted compliant electrodes and the fabrication of dielectric elastomer microactuators. His research interests include polymer-based microsystems and the development of new fabrication processes with these materials.

Muhamed Niklaus received the M.S. degree in physics from the Ecole Polytechnique Fédérale de Lausanne, Lausanne, Switzerland, in 2005, where he developed a theoretical model to describe configurations and scaling properties of DNA. Since 2006, he has been with the group of Prof. H. R. Shea at the Microsystems for Space Technologies Laboratory, Ecole Polytechnique Fédérale de Lausanne, working toward the Ph.D. degree in the field of nanocomplex produced by metallic ion implantation into polymers.

He develops an understanding of nanocomposites based on observations with high magnification microscopes such as SPM, SEM, TEM, etc. He is the coauthor of two international publications on the subject of ion-implanted electroactive polymers.

Massoud Dadras received the DEA degree from the Institute of Nuclear Science and Technology, Commissariat à l'Energie Atomique (CEA), France, in 1987, and the Ph.D. degree from the University of Orsay, Orsay, France, in 1990.

He has been with the Institute of Microtechnology, University of Neuchâtel, Neuchâtel, Switzerland, since 1991, where he is currently the Manager of Service for microscopy and nanoscopy. His research activities are oriented to the microstructural study and improvement of properties of thin layers used in microfabricated sensors, actuators, and microsystems.

Herbert Shea (M'00) received the B.Sc. degree in physics from McGill University, Montreal, QC, Canada, and the M.A. degree in physics and the Ph.D. degree (1997) from Harvard University, Cambridge, MA.

After two years as a Postdoctoral Fellow with the IBM T. J. Watson Research Center, he joined the Bell Laboratories, Lucent Technologies, Murray Hill, NJ, where he became the Technical Manager of the Microsystems Technology Group. Since April 2004, he has been an Assistant Professor with the Ecole Polytechnique Fédérale de Lausanne, Lausanne, Switzerland, where he founded the Microsystems for Space Technologies Laboratory. His current research topics include micromachined polymer MEMS (artificial muscles), ion micropropulsion, MEMS sensors for satellites, chip-scale plasma sources, and a 1-kg picosatellite to be launched in 2009.